A Scalable Synchronization Protocol for Large Scale Sensor Networks and Its Applications

Yao-Win Hong, *Student Member, IEEE,* and Anna Scaglione, *Member, IEEE,*

***Abstract*—Synchronization is considered a particularly difficult task in wireless sensor networks due to its decentralized structure. Interestingly, synchrony has often been observed in networks of biological agents (e.g., synchronously flashing fireflies, or spiking of neurons). In this paper, we propose a bio-inspired network synchronization protocol for large scale sensor networks that emulates the simple strategies adopted by the biological agents. The strategy synchronizes pulsing devices that are led to emit their pulses periodically and simultaneously. The convergence to synchrony of our strategy follows from the theory of Mirollo and Strogatz, 1990, while the scalability is evident from the many examples existing in the natural world. When the nodes are within a single broadcast range, our key observation is that the dependence of the synchronization time on the number of nodes N is subject to a phase transition: for values of N beyond a specific threshold, the synchronization is nearly immediate; while for smaller N, the synchronization time decreases smoothly with respect to N. Interestingly, a tradeoff is observed between the total energy consumption and the time necessary to reach synchrony. We obtain an optimum operating point at the local minimum of the energy consumption curve that is associated to the phase transition phenomenon mentioned before. The proposed synchronization protocol is directly applied to the cooperative reach-back communications problem. The main advantages of the proposed method are its scalability and low complexity.**

***Index Terms*—Communication systems, distributed algorithms, distributed feedback oscillators, sensor networks, synchronization.**

I. Introduction

MODERN advances in wireless technology, microelectromechanical systems (MEMS), and nano-scale sensors enable the development of large scale, low cost sensor networks. Each individual sensor now has the ability to simultaneously sense the environment, process data, store information and communicate with other sensors. These "swarms" of sensors can inform us about the physical world either directly or through the interaction among cooperating agents performing sensor fusion or distributed detection. Time synchronization plays an important role in various sensor fusion applications, such as the velocity measurement of a moving vehicle or the detection of temporally correlated data. For communication purposes, time synchronization is also crucial for the coordination among nodes in various multiple access techniques [2]–[5] or higher layer networking protocols. In order to minimize the cost and to extend the synchronization protocol to a large scale network, it is important to develop decentralized synchronization protocols that are both *simple* and *scalable*. Although many centralized synchronization protocols have been proposed, these methods are vulnerable to the failure of the central station, thus, prone to attack. They are obviously incompatible with the structure of sensor networks that are ad hoc and distributed in nature.

Recently proposed decentralized synchronization techniques [6]–[8] often require a large amount of message exchange or higher layer processing which may result in communication deadlock as the scale of the network grows. Interestingly, synchrony of periodic activities in autonomous systems are often seen in biological systems [9], physics, and chemistry [10]. One of the most popular examples is the synchronous flashing of fireflies [11] observed in certain parts of southeast Asia.[1] These biological systems do not operate under any complicated networking protocols or enforce any artificial engineering; yet, they have proven to be scalable with respect to the number of participants in the network. Conventionally, the biological systems that display synchrony are often modeled as a network of *pulse-coupled oscillators* (PCO). Using this model, the collective behavior of these large scale biological systems has been widely studied. One of the earliest analytical studies of these systems are done by Mirollo and Strogatz [1]. In their work, they proved the convergence toward synchrony for a network of pulse-coupled oscillators under the assumption of uniform coupling [1], noise-free environment and no delays between the firing and receiving of pulses. Models adopted in later work take into consideration the effect of nonuniform coupling [12] among oscillators, but still neglect the effect of delays. Others consider the effect of delays [13], [14], under the unrealistic assumption of a constant propagation delay between all nodes. Different behaviors have been observed in each of these scenarios, not all leading to synchrony. Although these complicated effects cause great difficulty in modeling the natural world, there are many degrees of freedom in designing a system that emulates the synchronization mechanism of natural networks.

The major contributions of this paper are: 1) we introduce an adaptive and distributed time synchronization method that emulates the strategy of synchronously flashing fireflies [11] and 2) we analyze the speed of convergence toward synchrony and find an optimum operating point for the network which achieves the best tradeoff between synchronization time and the energy

Manuscript received April 1, 2004; revised December 20, 2004. This work was supported in part by the National Science Foundation under Grant CCR-0347514 and in part by the Office of Naval Research (ONR) under Contract N00014-00-1-0564.

The authors are with the School of Electrical and Computer Engineering, Cornell University, Ithaca, NY 14853 USA (e-mail: yh84@cornell.edu; anna@ece.cornell.edu).

Digital Object Identifier 10.1109/JSAC.2005.845418

[1]Other examples of mutual synchronization in biological systems include the firing of pacemaker cells of the heart, the spiking of neurons, and the cycles of earthquakes.

spent to reach synchrony. Specifically, in each sensor node, we adopt the mechanics of the ideal PCO system in [1] and consider the application to UWB communications,[2] which are designed to generate pulsing signals that have small pulse durations compared with their duty cycle. However, in considering wireless networks, it could be disastrous to apply directly the strategy in [1], due to the many idealistic assumptions that are made in the model. Therefore, in this paper, we impose upon existing models [1] the realistic parameters of a wireless sensor network. In particular, we consider the path-loss attenuation, the propagation delay and the presence of noise, and we incorporate the pulse detection and the refractory period into the mechanics of the PCO, to adapt to these nonideal conditions. With this setup, we are able to construct practical pulse-coupling systems that converge to synchrony with modest performance degradations. From a networking perspective, the PCO system effectively eliminates the high-layer intervention and achieves time synchronization exclusively through the interaction at the physical layer. This falls into a larger class of systems that employs strategies inspired by mother nature (bio-inspired) to achieve scalable designs in large sensor networks, such as the physical-layer broadcasting system proposed in [15]. The system is invaluable to the application of large scale sensor networks due to its *decentralized structure* and its *simple mechanism*.

In our discussion on the speed of convergence toward synchrony, we will consider two network scenarios: 1) the case of a single broadcast domain, where the nodes are located within the broadcast range of one another and 2) the case of multiple broadcast domains, i.e., synchronization over multiple hops. The first case is analogous to the so called *all-to-all coupling*[3] [1] and the second one is similar to the case where nodes are subject only to local coupling [16].

In the design of distributed synchronization protocols, it is necessary to consider the scalability, energy efficiency, robustness and ad hoc deployment of large scale sensor networks [17]. The scalability of our scheme follows directly from the simple and distributed mechanics of the PCO, and from the large evidence existing in nature. In spite of the fact that the complexity of the PCO scheme is independent of the number of nodes N, we show that the synchronization time increases as $O(\log N)$ in the case of local coupling (c.f. Section V). In the all-to-all coupling case, we found that the synchronization time decreases as the number of nodes increases, and it exhibits a phase transition dropping to a value close to zero for $N > 1/\varepsilon$, where ε is the coupling strength (c.f. Section III). At the phase transition, an avalanche of pulsing occurs in the network where the nodes are synchronized successively in one shot. We provide insight on the *avalanche phenomenon* in Section V. In considering the energy efficiency, we calculate the transmission range that provides the best tradeoff between the energy consumption and the synchronization time (c.f. Section VI). The local minimum in energy consumption is due to the avalanche effect occurring at the phase transition point, where the number of pulses emitted to achieve synchrony is significantly decreased.

[2]We wish to remark that our method is applicable to a much wider class of transmitters.

[3]The case where the pulsing of one node imposes a coupling on all the other nodes in the network.

The advantage of the PCO scheme is that the precision of the synchronization process does not degrade over multiple hops due to the fact that the synchronization is achieved through a consensus among nodes and that the synchronization error is dominated by the propagation delay of the pulsing signal instead of the processing delay or the network congestion (c.f. Section VII). In contrast to our system, many existing systems, such as those proposed in [6] and [7], require one node to lock explicitly to the time scale of another node, in which case, the imprecision of the time estimate propagates and accumulates over multihops. In our system, the advantages due to mutual synchronization and physical-layer processing allows the time dispersion of the PCO protocol to be upper-bounded by the propagation delay throughout the network. Furthermore, the proposed strategy is adaptive and robust to time-varying network topologies in the sense that a new participant can be rapidly synchronized to the other nodes, and any number of the nodes leaving the network will not affect the achieved synchrony. All these features would be particularly valuable in numerous military wireless applications.

In this paper, we show that the PCO protocol can be directly applied to the *cooperative reach-back* problem, where we show that synchronization can either reduce significantly the dispersion or even lead to coherent superposition of the pulses when the signals have high fractional bandwidth and a reasonably long monocycle pulses [18]. In this case, the proposed method would provide array beamforming gains that increases significantly the range at which the sensor signals can be detected.

In the following section, we discuss briefly the existing network synchronization protocols and emphasize the advantages of our strategy.

II. Related Work

Over the years, many different time synchronization protocols have been proposed for distributed computer systems. Most of these protocols operate at the packet-level, where the time information is exchanged explicitly among nodes, and they require the processing of these messages to calibrate the time difference between nodes. The large majority of these schemes use point-to-point transmissions instead of capitalizing on the broadcast nature of the wireless channel and neglects the limitations that might occur in cheap sensor devices. For example, many systems utilize the Global Positioning System (GPS) [19] to synchronize the network to an external timescale. Even though this method achieves an accuracy in the order of 200 ns, it is expensive in terms of energy consumption and the cost of the hardware. It also requires a line-of-sight to the GPS satellite, which is unrealistic in many practical settings of the ad hoc network. Mills' network time protocol (NTP) [20] is the most widely used protocol in the internet. In the NTP, a hierarchy is constructed among nodes in the network with multiple roots synchronized to external global time sources and all the other nodes synchronized to its corresponding parent-node. Although the scalability and robustness of this system allows the NTP to be widely employed in the world of the internet, the accuracy is strongly affected by the symmetry of the delays in the transmission paths between the transmitter and receiver

node, and it also degrades significantly when the level of the node is low within the hierarchy.

Recently, there has been an increasing amount of studies on the synchronization and/or the timing of events in wireless sensor networks. In [6], the authors extended the NTP scheme to adapt it to the scale and the energy limitations of the wireless sensor networks, but the scheme proposed still exhibits the same loss in accuracy as the original NTP. In their experiments, a synchronization error of approximately 1 ms was observed even after eliminating the delay due to the channel contention in the medium access control (MAC) layer. In [8], a method is proposed to transform the local time estimate of an event into the estimate according to the time scale of another node. In this case, the chronology of events is generated at the local time scale of each node without the actual synchronization of the clocks. This scheme is suitable for sparse networks where full connectivity is not always guaranteed, and it achieves accuracy in the order of milliseconds. However, the accuracy of the time estimates also degrades with the increasing number of hops between two nodes.

In the reference broadcast synchronization (RBS) scheme [7], the nodes in the network are mutually synchronized to each other instead of locking to a global time clock. In this system, each node broadcasts, at the physical layer, their reference beacons to its neighbors. The nodes that received the beacon exchange with each other the arrival time of the beacon relative to the local clock and obtain a time difference matrix and clock skew information. Since each receiver experiences the same transmitter processing time, the difference of the locally estimated arrival time at each of these receivers will only contain the contribution from the clock difference while eliminating the contribution from the transmitter processing time. By exchanging these local timestamps, the accuracy of the RBS is improved by eliminating the dominant factors of the synchronization error due to the random processing time spent at the transmitter node, which may include the protocol processing and the variable delays of the operating system [7]. The RBS scheme requires a large amount of data exchange since each node needs to share the timing information of the received beacon signal with all the other nodes within the broadcast domain. Upon receiving these messages, the time difference matrix and the clock skew information relative to all nodes are processed and stored. These properties of the RBS makes it nonscalable to large scale sensor networks or networks with high node density. A multihop extension of this scheme was also described in [7].

The major advantage of the PCO synchronization strategy comes from the fact that it operates exclusively at the physical layer by transmitting pulses instead of packet messages. The mechanics of this synchronization scheme can also be implemented entirely with hardware at the frontend of the receiver. Therefore, the imprecision due to MAC layer delays, protocol processing or software implementation does not exist. Furthermore, the messages exchanged in the PCO scheme (the periodic pulsing signals) are independent of the origin of the signals since each received pulse is treated identically. This scheme requires no memory to store time information of other nodes and the synchronization is achieved on a global scale instead of calculating independently the relative time scale between every two nodes, as it is done in RBS [7]. Each node in the PCO network operates under identical mechanics, thus, the procedure adopted at each nodes is independent of the node identity and remains the same regardless of the number of nodes in the network. In the following section, we describe the mechanics of the PCO based on the model used in [1] and introduce the synchronization strategy that we derive from the characteristics of the network of PCOs.

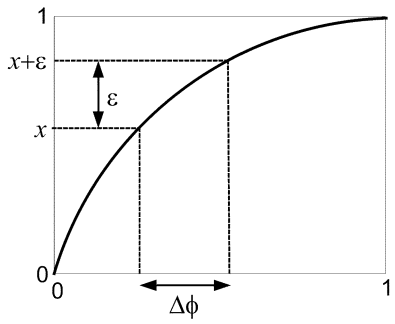

Fig. 1. Dynamics of a single PCO and the coupling due to pulsed interaction between nodes.

III. Synchronization Strategy With PCO

The distributed synchronization strategy that we propose is based on emulating the synchronization behavior observed in a population of pulse-coupled oscillators. In this paper, we adopt the model proposed in [1] and utilize the theoretical results within.

A. Pulse Oscillator Model and Network Dynamics

Consider a network of sensors each acting as a PCO. In our model of the PCO, each node in the network transmits replicas of a pulse signal $p(t)$ whose emission is controlled by an internal state variable $x(t)$ that can be viewed as the voltage potential in a resistor-capacitor (RC) circuit. As shown in Fig. 1, the state function $x(t)$ is a monotonic function increasing from its initial state to a threshold value at which point the accumulated charge within the RC circuit is released and a replica of the pulse signal $p(t)$ is transmitted (or fired). We assume, w.l.o.g., that the state variable $x(t)$ takes on values between 0 and the threshold 1. Specifically, define $x_i(t)$ as the *state function* of the ith PCO node. Assume that $x_i(t)$ is left-continuous and that it achieves the threshold value at time τ_i, i.e., $x_i(\tau_i) = 1$; at this instant, the node immediately emits a pulse $p(t)$ and resets the state variable to 0, i.e., $x_i(\tau_i^+) = 0$. If the node is isolated, meaning that no external signals are received from other nodes, then the state variable $x_i(t)$ follows a periodic pattern that increases as a smooth function of time, within each period, until it reaches the threshold 1 at which point the function is reset to 0. This results in the periodic emission of a pulse with period T, whose duration is equal to the time it takes for $x_i(t)$ to rise from zero to one. In particular, between the time τ_i^+ and $\tau_i + T$, where $x_i(\tau_i^+) = 0$ and $x_i(\tau_i + T) = 1$, the shape of the state variable is captured by the following function:

$$f_i(\phi_i) = x_i(\tau_i + \phi_i T), \quad \phi_i \in (0, 1] \tag{1}$$

which is called the *dynamics* of the oscillator i. We shall refer to τ_i as the firing time and ϕ_i as the *phase* of node i. As shown in (1), the duration of the pulsing period can be measured by the phase ϕ which is equivalent to normalizing the time between pulsing to the value 1. In this way, we avoid the discussion of the actual pulsing period measured in time when oscillators with different dynamics are used.

B. Coupling Between Pulse Oscillators

When the PCOs are not isolated, the interaction with other nodes can perturb the periodic pattern of their state functions as it is explained in the following. Assume that the nodes can receive signals only when it is not firing. In fact, the PCO is often assigned a duration of time right after its own firing, during which no signal can be received from other nodes. This period is referred to as the *refractory period* and it is asymptotically zero when the interaction is assumed to be instantaneous. The refractory period is crucial in maintaining the stability of the system since it prevents the occurrence of an infinite feedback (c.f. Section VII-A). When the signals arrive outside of the refractory period, the firing of an oscillator i will cause an increase ε_{ij} to the state function of every other node j, we refer to this increase as the *coupling* from node i to node j. In general, the coupling strength ε_{ij} may depend on many aspects such as the emission power of the pulse signal, the characteristics of the channel between i and j, and the arbitrary choices made at the receiver end. By properly choosing the coupling strength, e.g., inhibitory coupling $(\varepsilon < 0)$, we may obtain different complex behaviors, such as clustering or pattern generation in image processing [16], [21], in contrast to the global synchronization that we desire in this work. In this case, we are able to partition the network into distinct synchronized regions where each region is only synchronized within itself, while segregated from other partitions of the network. This extension is beyond the scope of this work and it is left for future work.

C. Synchronization of PCOs

We first consider the idealistic model [1] where the pulses from other nodes are received instantaneously and the coupling is independent of the node identities, i.e., $\varepsilon_{ij} = \varepsilon$ for all i, j. In this case, the pulse emission of node i at time τ_i changes the state variable of node j as follows:

$$x_j\left(\tau_i^+\right) = \begin{cases} x_j(\tau_i) + \varepsilon, & \text{if } x_j(\tau_i) + \varepsilon < 1 \\ 0, & \text{otherwise} \end{cases} \tag{2}$$

which means that either node j emits the pulse at the same time as node i (now and in the future) or node j will anticipate its own firing time because the residual rise necessary for the state variable $x_j(t)$ to reach the threshold 1 is smaller. Thus, only when the nodes emit the pulse simultaneously will they be insensitive to coupling and, therefore, behave as synchronous pulse oscillators. This coupling effect was also illustrated in Fig. 1, where an increase in phase has occurred due to the coupling on the state variable.

The model we described above has been used to explain different synchronization phenomena in large biological networks. In particular, it was used to explain the flashing of fireflies and the firing of pacemaker cells [1], whose periodic

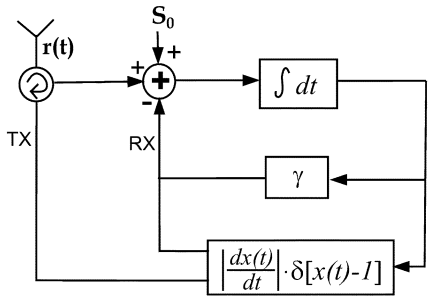

Fig. 2. Peskin's integrate-and-fire model considering instantaneous coupling, constant coupling strength, and no noise.

firing of pulses results in synchrony. We wish to remark that a more realistic model would incorporate variable levels of coupling, signal propagation delays and noise. The simplified model is equivalent to assuming that: 1) the pulse duration and propagation delay is short compared with the period T; 2) the path loss among node pairs has negligible differences and the nodes transmit the same power; and 3) the SNR is high. With the simplified assumptions that the coupling among nodes are identical and instantaneous, Mirollo and Strogatz have proven in [1] the following.

Theorem 1: [1, Th. 3.1–3.2]: For any positive coupling $\varepsilon > 0$, the set of initial states, $x_i(0)\ \forall i$, that never result in synchrony has measure zero, if the function f [defined in (1)] is *smooth*, *monotonically increasing* and *concave down*.

By neglecting the propagation delay and assuming that the nodes operate under the same dynamics, *every set of nodes that are mutually synchronized act as a single oscillator with the coupling strength equal to the sum of the couplings of all the nodes in the set*. This set of synchronously firing sensors are said to be *absorbed* by each other. The contribution of our paper is to explore the synchronous behavior of a network of interacting PCOs and utilize this property to achieve time synchronization in large scale sensor networks. In this paper, we utilize as dynamics, [c.f. (1)], the ones that are provided by the so called Peskin's Model [22].

D. Peskin's Model

The state function in the Peskin's model is defined by the following differential equation:

$$\frac{dx_i(t)}{dt} = S_0 - \gamma x_i(t), \quad 0 < x_i(t) < 1 \quad i = 1, \cdots, N \tag{3}$$

which is the well-known leaky integrate-and-fire model (IF). S_0 is a constant representing the speed of accumulation when there are no leakage and γ the leakage factor. Therefore, we have

$$f(\phi) = C(1 - e^{-\gamma T \phi}) \tag{4}$$

where $C = 1/(1 - e^{-\gamma T})$ and $T = \gamma^{-1} \ln[S_0/(S_0 - \gamma)]$. Note that the Peskin-type PCO, as mentioned in (3), can be implemented by a simple *RC* circuit as shown in Fig. 2, where the constant charge S_0 and the leaking component $-\gamma x_i(t)$ is sent into the integrator, while a pulsing occurs whenever $x_i(t)$ reaches the threshold 1. The pulsing is represented by the Dirac delta function $|(dx(t)/dt)|\delta[x(t) - 1]$, which integrates to 1 with respect to t after the time t^*, where $x(t^*) = 1$.

The behavior of the PCO protocol is only dependent on the normalized parameter ϕ, therefore, the pulsing period can be chosen arbitrarily according to the desired application. Given the number of periods needed to achieve synchronization, the rate of synchronization is obviously faster for small T. However, this leads to high energy consumption due to the frequent transmission of pulses. When the period T is large, on the other hand, the clock skew due to imprecisions of the hardware devices will cause the nodes to go out of phase before the next synchronization period. In other words, for a set of nodes that have a large clock skew, the synchronization pulse must be updated more frequently. Although the PCO protocol focuses on synchronizing the phase of the distributed clocks, the absolute time at each node can also be calibrated by simply broadcasting the GPS clock throughout the network, thus, achieving the clock accuracy up to the precision of the PCO protocol (c.f. Section VII).

In the numerical simulations throughout this paper, we will use, as the PCO dynamics at each node, the Peskin model with $S_0 = 5$ and $\gamma = 4.9$ unless mentioned otherwise.

The model described in this section is based on many ideal assumptions such as the instantaneous all-to-all coupling and the noise-free environment. These simplifying assumptions streamline some of the key steps necessary to prove in [1, Th. 1]. Even though synchrony has been found when these assumptions are relaxed, a more general proof is not available; it is extremely difficult to prove the convergence in a nonideal scenario, but nonetheless important to study it from an engineering point of view. In the following sections, we take into consideration the effect of noise and channel gain. We modify Fig. 2 to cope with these phenomena, and show, through simulations, how our strategy can still achieve synchrony within a finite accuracy.

IV. Pulse Detection

In the model considered previously, it was assumed that the system is noise-free. However, in practical scenarios, there exists thermal noise at the receiver front end and it is necessary for the sensor to distinguish between the received signal pulse and the channel noise. Therefore, we propose, in the following, a simple pulse detection scheme to achieve this goal.

Consider a network of N sensor nodes randomly placed in a specified region with a uniform distribution. Each node emits UWB monocycle pulses $p(t)$ with unit energy [23]. Due to the broadcast nature of the wireless medium, each node will receive a combination of pulses from other nodes with different gains and delays, therefore, the signal received at node i is

$$r_i(t) = \sum_q \sum_{\substack{n=1 \\ n\neq i}}^{N} A_{i,n}\sqrt{\mathcal{P}_n}\, p\left(t - \tau_n^{(q)} - \frac{d_{i,n}}{c}\right) + n_i(t) \quad (5)$$

where $n_i(t)$ is the ith receiver AWGN with variance N_0, $\tau_n^{(q)}$ is the emission time of the qth pulse emitted by node n, $\mathcal{P}_n$ is the power transmitted by node n, and $A_{i,n}$, $d_{i,n}$ is the channel gain and distance between nodes i and n. The channel gain $A_{i,n}$ is determined by the path loss model $1/d_{i,n}^{\alpha}$, where α is the path loss exponent ranging from 2∼4, and $d_{i,n}/c$ is the propagation delay, where c is the speed of light. Since the duration of the UWB pulse $p(t)$ is small compared with the pulsing period T, we assume that the received pulses do not overlap with each other such that each pulse adds an independent stimulus on the state variable. Since the theory of Mirollo and Strogatz (c.f. Theorem 1) proves that synchronization can be achieved in the case of uniform instantaneous coupling, the design of our receiver should be a function of the received signal such that an instantaneous uniform coupling occurs at the arrival of each pulse.

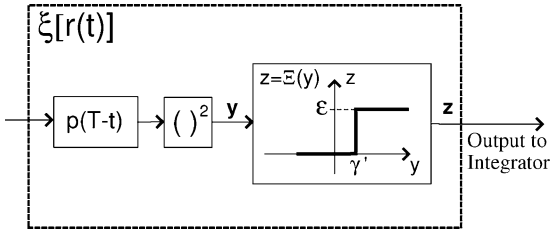

Fig. 3. Illustration of the pulse detection function $\xi[r(t)]$.

Let the received signal $r(t)$ be passed through a pulse detection function ξ, as shown in Fig. 3. The signal $r(t)$ is first passed through a matched filter followed by an energy detection whose output $y(t)$ is sent into a thresholding device. If the energy of the signal exceeds the threshold γ' at some time t^*, the output $z(t^*)$ of the thresholding device will take on the value ε; otherwise, the output is set to 0, i.e.

$$z(t) = \xi[r(t)] = \begin{cases} \varepsilon, & \text{if } y(t) \geq \gamma' \\ 0, & \text{otherwise} \end{cases} \quad (6)$$

where γ' is determined by the probability of false alarm. The output of the pulse detection function is then fed into the integrator of the PCO. In this case, only the detected pulses affect the state function of the receiving nodes. When the noise is not considered, the threshold γ' can be set to zero, thus allowing each sensor to accept coupling from all the other nodes in the network, i.e., all-to-all coupling. On the other hand, when the noise is nonzero and $\gamma' > 0$, the signals from far away nodes will fall below the threshold due to path-loss attenuation, thus limiting the effective range of the emitted coupling. However, the synchronization is still observed, through numerical simulations in Sections V and VI, even when the transmission range is limited, i.e., synchronization is achieved through multiple hops. The choice of γ' and the transmission power $\mathcal{P}$ affects both the reliability of the received coupling and the set of reachable nodes. Although the PCO protocol can be implemented with a simple energy detector, the choice is not optimal in general. In practice, the pulses that are emitted must have a nonnegligible duration, therefore, increasing the probability that the pulses will overlap. In this case, the optimum detector would allow a coupling of $\hat{N}\varepsilon$, where $\hat{N}$ is the maximum-likelihood estimate of the number of received pulses, which can be obtained through a complex generalized likelihood ratio test.

The threshold function $z = \Xi(y)$ can be chosen for different applications or be optimized over different cost functions. The specific example shown in Fig. 3 corresponds to the uniform coupling case that we assume throughout this paper. However, the choice of the coupling strength ε plays an important role in the speed of synchronization. In the extreme case where ε is greater than 1, the coupling from one pulse will immediately

trigger the other nodes to fire, the network can then be synchronized immediately upon the reception of the signal. This is exactly the case where a periodic beacon is transmitted from a base station to synchronize all the nodes within its broadcast range. Unfortunately, this system is less robust since the failure or mistake at the central node may cause a catastrophic failure in the synchronization process. Also, the receiver will be easily pushed out of phase by a single false alarm. On the other hand, if the coupling strength is small, synchronization can be achieved through multiple network iterations where no node has a dominant effect on any other node. In this case, the robustness is achieved with a significant increase of the locking time. Therefore, it is desirable for the coupling strength to reflect the reliability of the detections. Specifically, a more reliable detection resulting from a stronger signal should correspond to a stronger coupling and *vice versa*.

In the following sections, we neglect the effect of noise such that a better intuition can be derived from the results. However, the noise can be easily taken into consideration with the pulse detection strategy shown in this section.

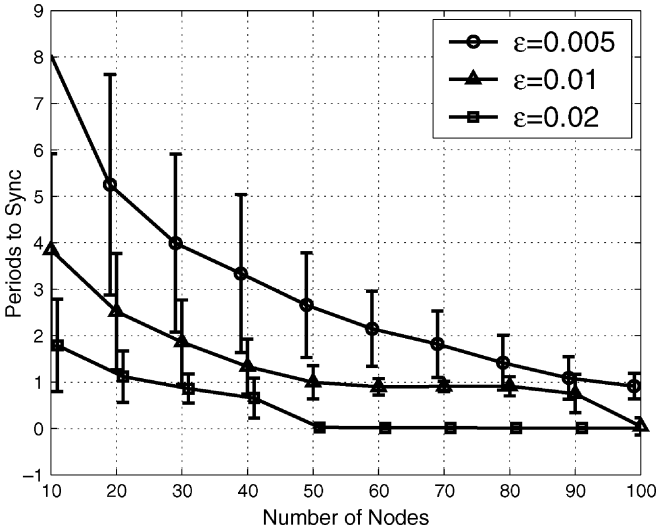

Fig. 4. Consider the case where nodes are within the broadcast range of each other. We show the number of period durations necessary to reach synchronization versus the number of users in the network.

V. Rate of Synchronization

As mentioned in Section II, the synchronization procedure of the PCO scheme does not require any buffering or calculations (other than the ones described in Fig. 2), therefore, the system is independent of the network size. Although the complexity of the protocol remains unchanged as the number of nodes increases, the average time required for the network to reach the synchronous state still depends on the number of nodes in the network.

We first look at the case where nodes are located within a single broadcast domain. Specifically, we consider a network of N nodes with all-to-all coupling and a coupling strength ε that is equal for all nodes. In this simulation, we do not consider the effect of noise or propagation delay, therefore, the emission of a pulse from one node will cause a constant coupling ε on all the other nodes at the time of the pulsing. We also consider all nodes to operate under the same dynamics as shown in Section III-D. The simulator is implemented as follows: first, we generate a random vector of the initial phase $\boldsymbol{\phi} = [\phi_0, \cdots, \phi_{N-1}]$, where each element is independent identically distributed (i.i.d.) uniform within [0,1]; then, we allow the node with the largest phase to fire first while updating the phase of other nodes with the elapsed time and the increase of phase due to the received coupling. This procedure is repeated until all the nodes in the network are synchronized, i.e., $\phi_i = \phi_j \; \forall i \neq j$.

In Fig. 4, we show the average locking time versus the number of nodes N for coupling strength $\varepsilon = 0.005$, 0.01, and 0.02, where the results are averaged over 1000 network realizations. The confidence interval (with the width equal to the standard deviation of the trials) shows that the convergence time depends largely on the initial phase of the nodes. From this study, two important observations can be made: 1) the number of cycles to reach synchrony decreases as the number of nodes and/or the coupling strength increases and 2) there is a phase transition at the point $\varepsilon N = 1$ where the synchronization is achieved almost immediately.

It is evident from the PCO model (in Fig. 1), that a large coupling strength, ε, would increase the synchronization speed since the number of nodes that are synchronized is also increased. Even when the nodes are not synchronized immediately, the anticipated pulsing time will be reduced due to the coupling, thus reducing the phase difference between the pulsing node and the other nodes in the network. In this case, the number of steps required to reach the same phase is smaller if each step ahead is larger. The relationship between the rate of synchronization and the number of nodes follows similarly. In fact, increasing the number of nodes, indirectly, increases the frequency of the coupling contributions. However, since the dynamics are nonlinear, amplifying the coupling strength is not equivalent to adding up coupling signals which are separate in time—the two are equivalent only if they are received exactly at the same time. In the latter case, the nodes that fire simultaneously are considered as being "absorbed" into one equivalent node whose pulses cause twice the coupling intensity. This implies that the functional dependence of the rate of synchronization with respect to N and ε are related but not exactly identical.

Even more remarkable is the existence of a phase transition at the point $\varepsilon N = 1$, where an abrupt transition of the synchronization time occurs, sending the locking time to a value close to zero, as observed in Fig. 4. In Fig. 4, the locking time decreases significantly at the points $N = 50$ and $N = 100$ for the curves representing the coupling strength of $\varepsilon = 0.02$ and $\varepsilon = 0.01$, respectively. It is not by coincidence that the critical phase transition occurs at the points where $\varepsilon N = 1$.

Claim 1: The phase transition of the synchronization time with respect to N occurs at the point where $\varepsilon N = 1$.

To better understand this effect, let us consider a deterministic scenario, as shown in Fig. 5, where the initial phases of the N nodes, $\boldsymbol{\phi}(0) = [\phi_0(0), \phi_1(0), \cdots, \phi_{N-1}(0)]$, are assigned the values $\phi_i(0) = 1 - i\varepsilon$, for $i = 0, 1, \cdots, N-1$. Assume that the dynamic f of the oscillator is a linear function such that

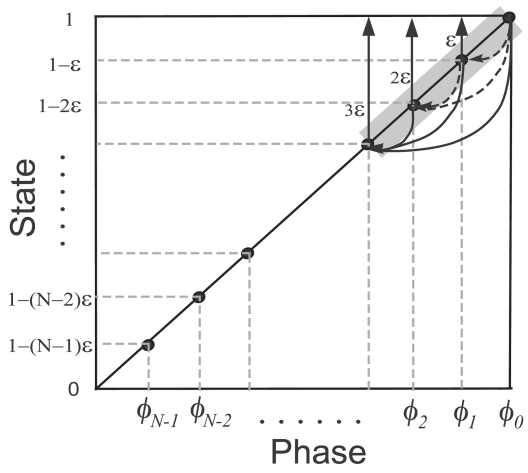

Fig. 5. Phase of N nodes are uniformly spaced by $\varepsilon = 1/N$ within the interval [0,1]. The nodes within the shaded area are absorbed into one equivalent node with coupling strength proportional to the number of nodes in the area.

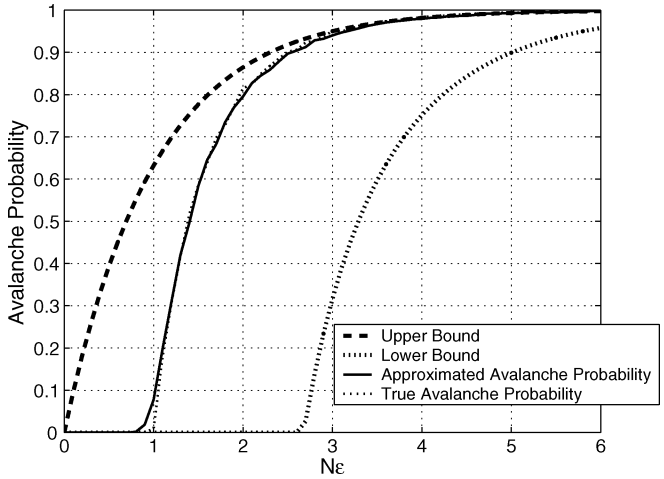

Fig. 6. Upper and lower bounds to the avalanche probability of the approximate model for a network of N nodes.

$f(\phi) = \phi$, then, the state value $x_i(0) = \phi_i(0)$, for all i. Since $\phi_0(0) = 1$, the state x_0 of node-0 reaches the threshold and immediately emits a pulse that imposes a coupling ε upon all the other nodes within the network. Since node-2 was originally at the state $x_2(0) = 1 - \varepsilon$, the firing of node-1 will necessarily move the state of node-2 to $x_2(0)+\varepsilon = 1$, thus triggering node-2 to fire as well. When node-2 fires, node-3 moves also to the state $x_3(0)+2\varepsilon = 1$ and fires. Continuing in this fashion, the successive pulsing leads to an *avalanche effect* that immediately locks the network to synchrony. Since the coupling is assumed to be instantaneous, all the nodes are actually firing simultaneously, therefore, achieving synchrony instantaneously.

In order to justify Claim 1, we assume that the initial node phases $\boldsymbol{\phi}(0)$ are Poisson points in the interval [0,1] with average frequency $\lambda = N$; using initial random phases that are uniformly distributed in [0,1] would have been more logical but it would have made our derivations quite cumbersome. More specifically, we set $\phi_0(0) = 1$ (i.e., the node with index zero is at its firing time) and let $\phi_i(0) = 1 - \sum_{j=1}^{i} \tau_i$, where $\{\tau_1, \cdots, \tau_{N-1}\}$ are i.i.d. $\sim \text{Exp}(N)$.

For any $0 < \varepsilon < 1$, let us define the events

$$E_i = \{\tau_1 + \tau_2 + \cdots + \tau_i < i\varepsilon\} \quad \forall i = 1, \cdots, N-1.$$

Considering the case of linear dynamics (see Fig. 5), the avalanche event $\equiv \bigcup_{i=1}^{N-1} E_i$. We justify our claim by proving the following lemma (the proof is provided in the Appendix).

Lemma 1: Let τ_i be an exponential random variable with parameter λ, for $i = 1, \cdots, N-1$, and let $\tau_0 = 0$. The following bounds hold true:

$$\max\{A, 0\} \le \Pr\left\{\bigcap_{i=1}^{N-1} E_i\right\} \le 1 - e^{-\lambda\varepsilon} \tag{7}$$

where

$$A = \begin{cases} 1 - \frac{\lambda\varepsilon e^{-\lambda\varepsilon+1} - [\lambda\varepsilon e^{-\lambda\varepsilon+1}]^N}{1-\lambda\varepsilon e^{-\lambda\varepsilon+1}}, & \text{for } \lambda\varepsilon \ge 1 \\ -(N-2), & \text{for } \lambda\varepsilon < 1 \end{cases}. \tag{8}$$

In Lemma 1, we obtained the bounds for the avalanche probability of the approximated model for the distribution $\sim \text{Exp}(\lambda)$. With the upper and lower bounds, we can see that, for $N\varepsilon \ll 1$, the avalanche probability is upper-bounded by $1 - e^{-N\varepsilon} \approx N\varepsilon \ll 1$ and, for $N\varepsilon \gg 1$, the probability is approximately equal to 1. This is verified in Fig. 6, where we show the avalanche probability for the case $\lambda = N = 100$, along with the bounds obtained in (7). The avalanche probabilities for the approximated model and the more realistic model with uniform phase distribution have negligible differences, which shows the accuracy of our approximation. As expected, the probability of the avalanche occurs with high probability when $N\varepsilon > 1$, while the probability is small otherwise. We note that, in the model described in Section III, the dynamics f is concave instead of linear as described above. In this case, the nodes that are absorbed due to the sum coupling strength $m\varepsilon$, for $m = 1, \ldots, N$, have initial phases within the interval $[f^{-1}(1 - m\varepsilon), 1]$. Since f^{-1} is convex upwards, the area corresponding to the initial phases that are absorbed is larger than $[1 - m\varepsilon, 1]$ and the avalanche will occur with a higher probability.

Although the locking time decreases with N when the nodes are located within the same broadcast domain, the opposite is true when the synchronization process is applied over nodes that can only receive coupling signals from their near neighbors (the multihop scenario). This scenario arises in practice when the path loss effect causes the received signal to fall below the detection threshold for a distant receiver. Although the random effect of the channel gain may cause close-by nodes to also fall below the detection threshold, we consider in our simulation model the case that all nodes within the transmission range receive the signal perfectly, while those outside the transmission range do not receive the signal at all. In Fig. 7, we considered the case of N nodes randomly distributed, with the uniform distribution, in a $d \times d$ (m^2) square area, and the initial phase of each node is uniformly distributed between [0,1]. In this case, we fix the coupling strength to $\varepsilon = 0.01$ and the node density to $N/d^2 = 0.4$ nodes/m^2 for all network realizations. In Fig. 7, we show that the locking time increases with the scale of the network for the cases where the transmission range r of each

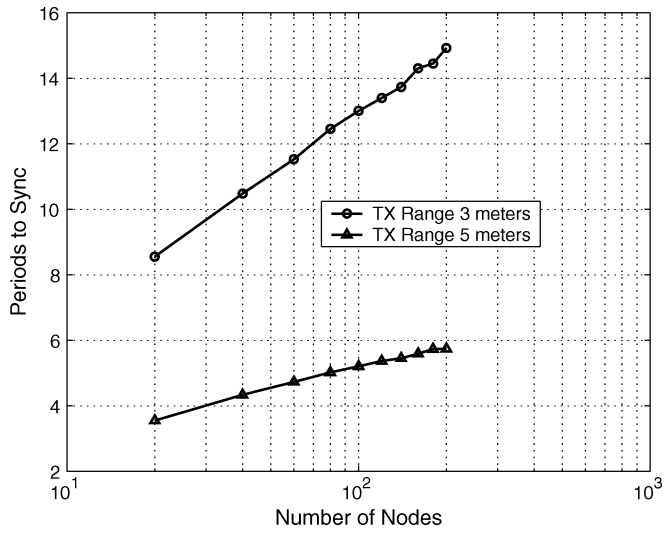

Fig. 7. Locking time versus the number of nodes in the network when the transmission range is limited to $r = 3$ and $r = 5$, and the node density is equal to 0.4 $\mathrm{nodes/m^2}$.

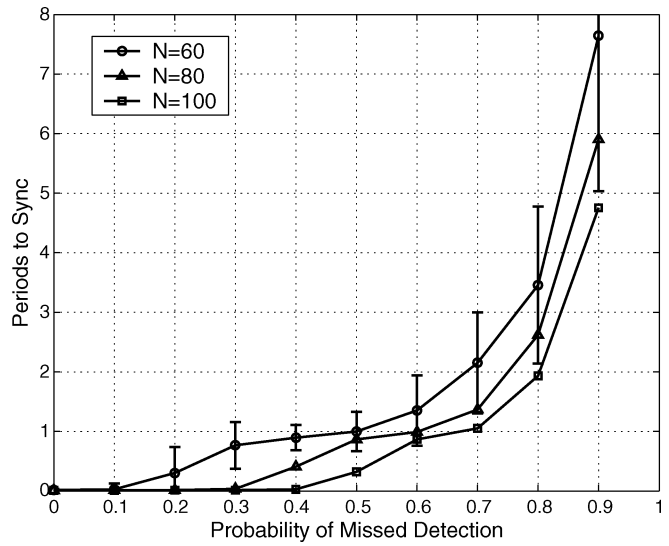

Fig. 8. Locking time versus the probability of missed detection for a network with all to all coupling and $\varepsilon = 0.02$.

node is limited to 3 and 5 m, respectively. We can see that the increase in locking time is approximately in an $O(\log N)$. Since the node density is fixed, the average number of nodes that each transmitter can reach is also fixed, therefore, it is unlikely to experience the avalanche effect that we discussed previously as long as $\varepsilon N(r) \ll 1$, where $N(r)$ is the number of nodes located within a single broadcast domain. However, if $\varepsilon N(r) \approx 1$, the immediate synchronization was also observed, even though the transmission range is limited (c.f. Fig. 9 in Section VI).

Sync Rate With Detection Error: Considering the effect of noise, the detection threshold, as indicated in Section IV, should be chosen such that the probability of false alarm is sufficiently small and, thus, negligible. Neglecting false alarms, we study the rate of synchronization by considering only the missed detections. Using the same simulator as that of Fig. 4, we show in Fig. 8 the average locking time versus the missed detection probability. For $N = 60$, 80 and 100, and $\varepsilon = 0.02$, we show that the locking time increases with respect to the probability of missed detection and that an avalanche occurs when the probability of missed detection is less than $1 - 1/N\varepsilon$, corresponding to the approximate missed detection probabilities of 0.2, 0.4, and 0.5, for $N = 60$, 80, and 100.

With the approximate model used in Lemma 1, we can analyze also the effect of noise on the avalanche probability for a given missed detection probability p_{MD}. The bounds in Lemma 1 hold true even when there are missed detections with probability p_{MD} by simply setting $\lambda = (1 - p_{MD})N$. In fact, a Poisson process with average frequency λ which is tagged with probability $(1 - p_{MD})$ is well known to be a Poisson process with parameter $(1 - p_{MD})\lambda$. This leads to the following.

Claim 2: For a probability of missed detections equal to p_{MD} the phase transition of the synchronization time with respect to N occurs at the point where $\varepsilon N(1 - p_{MD}) = 1$.

This is intuitively true since the missed detection of pulses will not contribute to the coupling strength, thus, requiring a larger coupling strength per pulse to achieve the same avalanche as in the noiseless case. This strengthens the result that we obtained from Fig. 8.

Remark 1: As mentioned in Section III-D, the choice of the pulsing period is arbitrarily determined according to the application. For the example in Fig. 4, the time to synchronize a network of 40 nodes is equal to 3.2, 1.3, and 0.75 pulsing periods for $\varepsilon = 0.005$, 0.01, and 0.02. If a fast synchronization is required, one cycle period can be chosen to be sufficiently larger than the round-trip delay of two synchronizing nodes, e.g., in the order of μs. Operating at this pulsing frequency requires a large energy consumption, which is undesirable for sensor network applications. When the speed of the synchronization is not crucial, one may allow pulses to be emitted every few hours. However, the manufacturing imprecision can cause errors in the way the state variable is updated and it is reasonable to think that the error will accumulate over time, making it undesirable to have long periods between successive synchronization pulses. These type of imprecision are hardware dependent and are difficult to capture in our simulations. In practice, it is important to choose a pulsing period which leads to the right compromise between assuring that the nodes phases are locked accurately and avoiding the waste of energy.

In this section, we have shown that the power for the pulse transmission has a monotone relationship with respect to the locking time: the increase of power results in a larger broadcast range and, thus, a shorter locking time while a smaller broadcast range leads to a longer locking time. However, the relationship between the synchronization time and the total energy consumption of the system to achieve synchrony is more complex. This is the subject of the following section.

VI. Energy Efficiency Versus Locking Time

Intuitively, energy efficiency in the transmission system is associated to a decreased transmission power at each node or a reduced number of transmissions. In achieving network synchronization, it may not always be desirable to reduce the transmission power since an arbitrarily small power would require more pulses to be emitted before the synchronous state

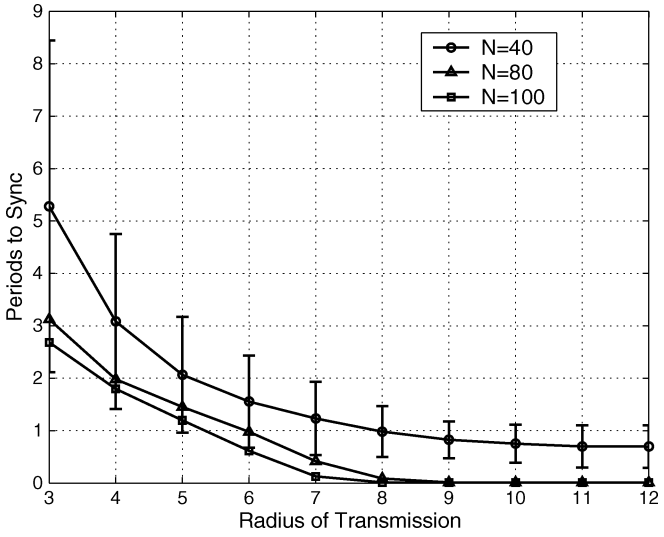

Fig. 9. Average time necessary to reach synchronization with respect to the transmission range.

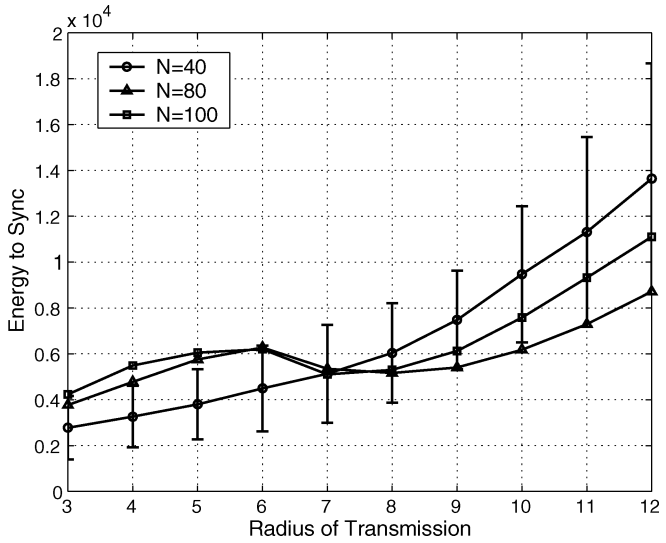

Fig. 10. Average total energy consumption of the entire network to reach synchronization with respect to the transmission range.

can be reached. In this case, it is not trivially determined which values of the transmission power would lead to less energy consumption. In the following, we discuss the tradeoff between the total energy consumption versus the synchronization locking time under the ideal assumptions of uniform and instantaneous coupling.

We consider the case where N nodes are randomly distributed with the uniform distribution in a 10×10 m^2 network area and the coupling strength $\varepsilon = 0.02$ for all nodes. The results are averaged over 1000 realizations of the network topology and the initial phases. In Fig. 9, we show the locking time over different values of the transmission range for the number of nodes $N = 40$, 80, and 100. The confidence interval is shown only for $N = 40$ to maintain the clarity of the figure. We observe that the locking time decreases as the transmission range increases since the number of nodes $N(r)$ that are within the same broadcast range increases, as shown in Section V. We note that the area of the single broadcast region is defined such that every pair of nodes within the region has a direct link between each other. In this case, the single broadcast region is exactly the circular region with the diameter equal to the transmission radius, thus, the area of the region is equal to $\pi r^2/4$. Specifically, for the case of $N = 80$ uniformly distributed in the 10×10 square region, we have $\varepsilon N(r) = 0.02 \cdot (80/(10 \cdot 10)) \cdot (\pi r^2/4)$ such that $\varepsilon N(r) \approx 1$ for $r = 8$. Similarly, for the case of $N = 100$, we have $\varepsilon N(r) \approx 1$ when $r = 7$. At these points in Fig. 9, the locking time decreases to a value close to zero since the avalanche effect allows the network to synchronize immediately when $\varepsilon N(r) \approx 1$ in a single broadcast region.

Note that the transmission range is determined by the transmission power and the path loss. Therefore, by considering a path-loss exponent equal to 2, increasing the transmission radius by a factor of b requires the transmission power to increase by a factor of b^2. We note that a small transmission power requires more pulses to be emitted before synchrony is achieved, therefore, choosing a small transmission power will not necessarily result in a lower energy consumption. In the simulations of Fig. 10, we count the total number of pulses emitted by the entire network of nodes before synchrony is achieved. Multiplying this number by r^2, the square of the transmission radius, we obtain the total energy consumption normalized by the energy of a single pulse necessary to reach a transmission range equal to 1. When the node density is high, the total energy consumption shows a local maximum and a local minimum in the curve; when the nodes density is low, the total energy consumption increases monotonically with respect to the energy of a single pulse, i.e., the transmission range. Remarkably, the local minimum occurs at the point of phase transition that we described in the previous section. At this point, the number of pulses emitted before synchrony is reduced significantly, therefore, reducing the total energy consumption. After this point, the number of pulses does not decrease much further, therefore, causing an unnecessary increase in energy consumption when we increase the pulse energy.

Although a trend in Fig. 10 shows that a lower energy consumption can be obtained with a smaller transmission power, the connectivity may be easily lost in this case. (The range values chosen in the simulations allow over 85% of the network realizations to be fully connected.) Even when the connectivity is guaranteed, the synchronization time may still be unaffordable. In Fig. 11, we combine Figs. 9 and 10 to obtain the relationship between the total energy consumption and the synchronization time. We observe that one should choose the operating point at the local minimum, when it exists, so that the synchronization can still be achieved rapidly even when it consumes only a low amount of energy. This point corresponds to the local minimum in energy consumption shown in Fig. 10. However, this point may not exist when the network has always $\varepsilon N(r) < 1$, as is the case for $N = 40$ in Fig. 10.

Interestingly, the energy-time tradeoff can also be observed in most of the existing synchronization schemes. In the packet-level synchronization protocols, increasing the transmission power also increases the area covered by a single broadcast range. Therefore, more nodes can be reached through

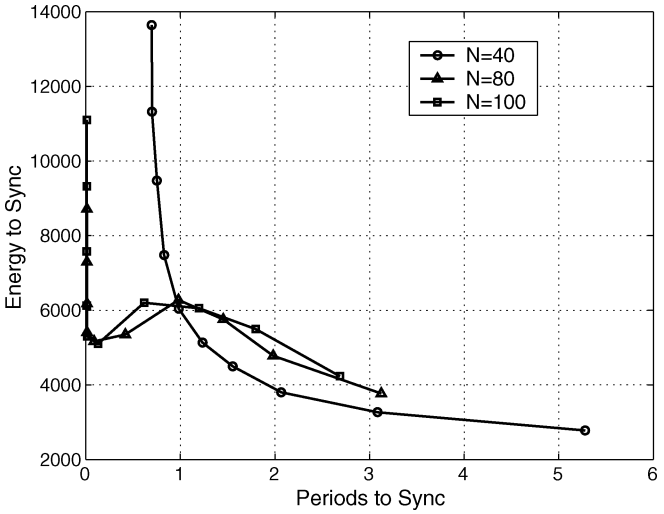

Fig. 11. Average total energy consumption of the network to reach synchronization versus the time needed to reach synchronization when $\varepsilon = 0.02$.

a single hop. On the contrary, reducing the power results in an increased amount of relay transmission and also reduces the precision of the synchronization in many schemes [6], [7].

VII. Synchronization in Nonideal Environments

The protocol proposed in this paper is based on the simplified models that are used to explain the synchronous behavior of many biological systems. However, these simplified models cannot be applied directly to the wireless network without modifying the strategy to take into consideration the characteristics of a wireless channel and the nonideal variations in the sensor devices. In addition to that shown in Section IV, we introduce a number of modifications to the basic model in Fig. 2 to address the nonideal conditions that may arise in the physical transmission medium and at the receiver. We show numerically, in this section, that the system that is proposed converges to synchrony with modest performance degradations.

A. Propagation Delay and Multipath Considerations

The ideal PCO model shown in Section III assumes that a sensor node cannot receive coupling from other nodes at the time it is firing, i.e., the transmission is half-duplex. Therefore, the set of nodes that are synchronized to each other do not impose a coupling on one another. However, this is based on the assumption that the coupling occurs instantaneously, which falls short when the propagation delay is considered. In this case, the set of nodes that are initially synchronized would impose a coupling among one another, causing the sensors to pulse continuously without rest. For example, consider a network with N nodes and all-to-all uniform coupling with a sufficiently large coupling strength, e.g., $\varepsilon = 2/N$. When the nodes are initially synchronized, they will emit a pulse simultaneously upon reaching the threshold in the state. In the presence of propagation delay, each node will receive the coupling from all the other nodes since the arrival of these pulses would not collide with the transmission of the receiving node. The sum of the coupling strength will cause the receiving node to reach the threshold immediately, thereby, transmitting another pulse right after the previously emitted pulse. This occurs repeatedly, causing the nodes to emit pulses continuously without stop and, thus making the system unstable.

To prevent the system from being unstable, it is necessary to assign a rest period right after the pulsing of a signal, where the receiver is shut off and all the signals arriving within this period are ignored. We conjecture that this is the functionality of the period that is often referred to as the *refractory period* in biological systems. Since the pulses that arrive during the refractory period do not change the nodes' states, the protocol cannot ensure a precision greater than the value of the refractory period $\Delta\tau$. By appropriately choosing the duration of the refractory period, the system can be stabilized such that the nodes will converge to the state where they all pulse periodically with the period T and with a phase that remains within the precision $\Delta\tau$. Therefore, as in [24], we define a new notion of stabilized synchronization as follows.

Definition 1 (Stabilized Synchronization): A PCO network reaches a **stabilized synchronization** with pulsing period T and precision δ if and only if the following conditions are satisfied.

1) For all i, there exists q_i such that, for all $q > q_i$

$$\left|\tau_i^{(q+1)} - \tau_i^{(q)}\right| = T \tag{9}$$

where $\tau_i^{(q)}$ is the qth firing time of node i.

2) For all $i \neq j$, there exists q_i, q_j such that for any n a positive integer

$$\left|\tau_i^{(q_i+n)} - \tau_i^{(q_j+n)}\right| < \delta. \tag{10}$$

Claim 3: For any PCO network within a single broadcast domain, there exists a refractory period $\Delta\tau$ such that the stabilized synchronization is achieved with the precision $\Delta\tau$.

Claim 3 is justified by the fact that the protocol, guided by exactly the same dynamics as in Theorem 1, cannot reach rest until all the nodes are receiving pulses in the refractory period. Instead, when this happens, the pulse emissions no longer perturb the states of any of the nodes, implying that stabilized synchronization is achieved. A consequence of Claim 3 is that the maximum dispersion of the synchronization process is upper-bounded by $\Delta\tau$ (the *maximum dispersion* [7] is defined as the maximum phase difference between the nodes in the network).

Claim 4: For a PCO network in a single broadcast domain with pulse duration ω, delay spread θ and maximum round-trip delay $2d_{max}/c$, where d_{max} is the maximum distance between any two nodes in the network and c the speed of light, the choice of the refractory period $\Delta\tau = \omega + \theta + 2d_{max}/c$ achieves the stabilized synchronization.[4]

Suppose that the area that is reachable within the transmission range of a single sensor (i.e., a single broadcast domain) is sufficiently large such that the choice of the refractory period $\Delta\tau$ is dominated by the maximum distance between any two nodes in the domain, i.e., d_{max}. Even when the network is much larger than the reachable distance of a single transmitter, it is sufficient

[4]When the PCO is implemented in the application layer instead of the physical layer, one should also include the processing delay into the refractory period.

to choose $\Delta\tau$ proportional to the maximum round trip delay of the nodes located within their transmission range (which is limited by the path loss and the coupling threshold introduced in Section IV). This choice of the refractory period is sufficient to avoid the case of instability, as indicated earlier, since a node outside of the transmission range can only be reached through multiple hops and does not create the direct feedback that causes the instability.

In evaluating the performance of a locally connected network, we consider a simple topology where the nodes $s_1, \ldots, s_N$ are aligned in order in one dimension and uniformly spaced by a distance d. Suppose that the transmission of each node can only reach its closest neighbors and that each node in the network operates under the same dynamics with the pulsing period T and the refractory period $\Delta\tau$. From Claim 3 and from the assumption that only the two adjacent nodes are within the same broadcast domain, we can assume that, after synchronization, the phase of node i is a random value with a uniform distribution in $2\Delta\tau$ centered at the phase of node $i-1$. Let $u_i = \tau_i^{(q_i+n)} - \tau_{i-1}^{(q_{i-1}+n)}$, where $\tau_i^{(q_i+n)}$ is as defined in (10); then the dispersion $D_{1,N-1}$ between node 1 and node $N-1$ is equal to the sum of random variables $D_{1,N-1} = u_2 + \cdots + u_{N-1}$ whose variance is equal to $(N-1)\Delta\tau^2/3$. Because $\Delta\tau \geq 2d/c$, the standard deviation of the dispersion is $O(\sqrt{N-1})$. In contrast, if all the nodes were in the same broadcast domain, the maximum round-trip delay would have been $2(N-1)d/c$; by assuming that the dispersion is uniform around the phase of node 1, the standard deviation of the dispersion $D_{1,N-1}$, in this case, is $O(N-1)$. This means that the multihop network performs a more accurate synchronization compared with the single-hop case.

Remark 2: We note that the precision of the synchronization process is improved by limiting the transmission range of each node. This is counterintuitive since the precision of most synchronization protocols applied in multihop scenarios degrades due to the error propagation [6], [7]. We shall point out that this improvement is attained as long as the dominant source of imprecision for the PCO synchronization is the propagation delay and not the processing delay. The latter can be reduced significantly by implementing the PCO as a simple analog hardware device. Note that the processing delay is typically the dominant cause of imprecision for most synchronization protocols that operate at higher layers [6], [7], [20], while the propagation delay is often neglected (see, e.g., [7]). Hence, our imprecision is in the order of the delays that the other methods neglect. While the maximum round-trip delay is reduced by having a smaller transmission range, the processing delay is fixed and independent of the network connectivity so there is no benefit in reducing the range of transmission and, in fact, the only phenomenon observed is that of error accumulation.

Consider three network scenarios with the number of nodes $N = 10$, 40 and 90, and that they are uniformly distributed in a square area of 5×5 m^2, 10×10 m^2, and 15×15 m^2, therefore, all have the same node density. Similarly, we neglect the pulse duration and the delay spread, and assume that the initial phases are uniformly distributed within [0,1]. In Fig. 12, we show the evolution of the maximum dispersion with respect to the time in units of periods and show that it decays with time converging toward the synchronization within a $\Delta\tau$ precision. With the transmission range of each node fixed to be 5 meters, the network becomes multihop as the area increases. We show that even in the multihop setup, the performance of our synchronization scheme is not degraded with respect to the single-hop scenario. At the time equal to 10.5 periods, the maximum dispersion is equal to 8.68, 14.2, and 21.3 ns for each of the previously mentioned scenarios, which are all bounded by the precision of considering a single broadcast domain over these networks, i.e., $\Delta\tau = 47.3$, 94.2, and 141.4 ns.

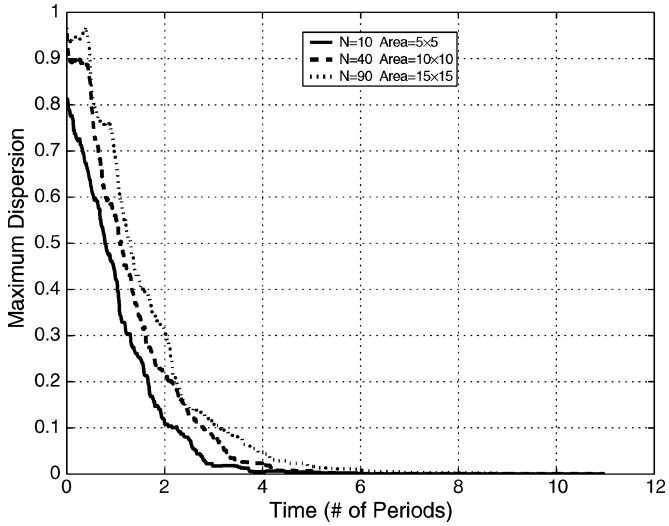

Fig. 12. Evolution of the maximum dispersion with respect to the time in units of periods.

We note that the relationship between the locking time and the synchronization precision of the PCO scheme is similar to that of the RBS system. In RBS, increasing the number of reference broadcasts may tighten the eventual synchronization due to averaging over the different packets. However, increasing the number of broadcasts implies the increase in the locking time as well. Similarly, from the argument above, the PCO scheme can achieve a higher precision if the transmission range is smaller. But, a smaller transmission range would result in a longer synchronization time, thus, presenting the same tradeoff as that observed in RBS.

B. Variations in the Intrinsic Frequency

In previous discussions, we assumed that the oscillators operate under identical dynamics, where the function f_i in (1) is such that $f_i = f$ for all i. However, there are always slight variations in the realistic devices causing an offset in the oscillating frequency (or referred to in other cases as the clock skew). Consider a set of nodes in a single broadcast domain with $N = 80$ and $\varepsilon = 0.1/N$. The normalized pulsing period is randomly chosen with a uniform distribution within the interval [0.9,1.1]. In Fig. 13, we show the evolution of the pulsing instants for a particular realization of this scenario. We observe the convergence to synchrony when the variation in frequency is of a modest amount such that the coupling from other nodes can overcome this difference in the oscillators internal dynamics. In all our numerical trials under this scenario, we observe the convergence to synchrony in all realizations that were generated.

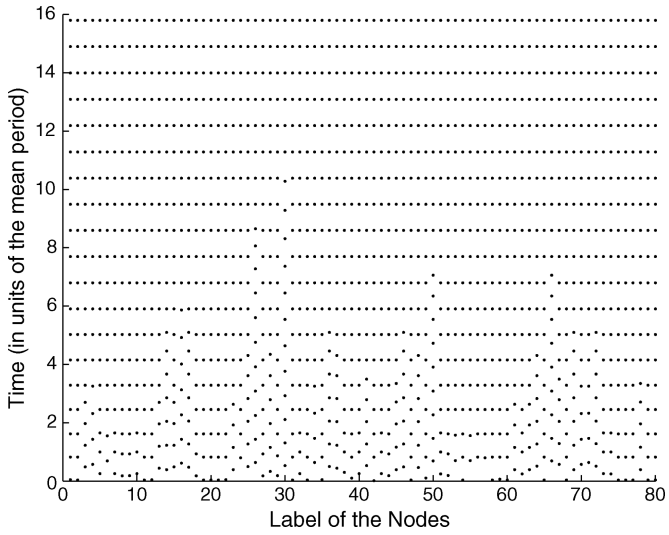

Fig. 13. Example of the synchronization process when the set of nodes have different pulsing periods uniformly distributed between [0.9,1.1].

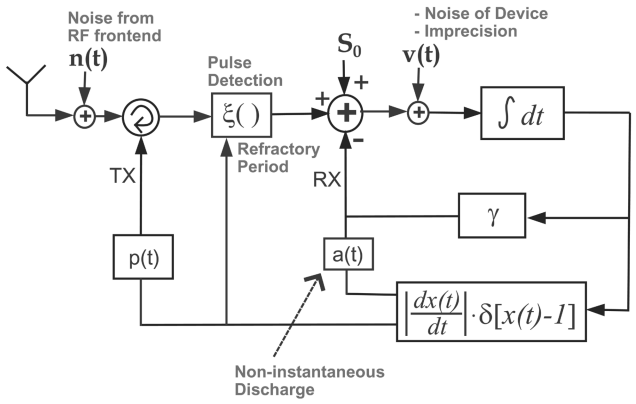

Fig. 14. Peskin's model considering the realistic channel effects, dispersion and propagation delay, noninstantaneous coupling, and noise.

There may be numerous variations in the oscillating device such as the rate of self-accumulation S_0 or the speed of leakage γ. Even an internal noise in the feedback loop of the oscillator may affect the pulsing period. These nonidentical device parameters caused by manufacturing defects may cause the nodes to pulse at different times or go out of phase easily, even when the nodes are initially synchronized. However, when the variation of the devices are small and the coupling strength is properly chosen, the interaction between nodes will trigger a node to fire even when the self accumulation state of that node is still a small amount away from the threshold. Therefore, the coupling strength overcomes the small variations due to hardware implementation.

In considering the realistic parameters of a wireless communication channel, the model of the PCO device is modified, as in Fig. 14, to adapt to these nonideal environment. The filters $p(t)$ and $a(t)$, in Fig. 14, correspond, respectively, to the finite-pulse duration and the noninstantaneous discharging of the potential stored in the device. All the parameters that disagree with the assumption of instantaneous coupling, including the propagation delay and multipath, can be dealt with by increasing the duration of the refractory period. Similar to that in Fig. 2, the block $|(dx(t)/dt)|\delta(x(t)-1)$ represents the thresholding of the state variable such that a pulse is emitted when $x(t)=1$. The output is fed into the pulse detection function ξ to signal the beginning of the refractory period. While we utilize the pulse detection function ξ to reduce the effect of noise at the RF frontend, the joint effect of internal noise and frequency offset $v(t)$ is not treated explicitly. Similar to the case of intrinsic frequency variations, these small defects can be overcome by the interaction among nodes with a sufficiently large coupling strength.

C. Dynamical Networks

The robustness of the system in a highly dynamic network is evident from the strategy that we propose. Since the synchronization process is independent of the identity of the coupling signals, the same strategy can be adopted in a highly dynamic network without special considerations on the original synchronization procedure. Considering the case where a small number of nodes (relative to the number already in the network) randomly join or drop out of the network. Since the number of nodes already synchronized is dominant over the number of new nodes, the sum of the coupling from synchronized nodes will trigger the new nodes to fire immediately, while remaining synchronized to each other without a shift in phase of its firing instants. When the number of new nodes is large, the network will converge to a new synchronization equilibrium, but the synchronization is still assured. Furthermore, the PCO strategy does not depend on the topology of the network, therefore, the mobility of the node does not affect the convergence.

VIII. Cooperative Reach-Back Application

In this section, we utilize the PCO scheme to synchronize the transmission of the sensor nodes to achieve beamforming gains that can reach a far destination. This effectively solves the so called *cooperative reach-back problem*. The key idea of this work is to incorporate the source data into the dynamics of the source oscillator.

Consider the case where the network intends to send data to a remote receiver that the nodes are not able to reach individually without consuming rapidly their power supply. In achieving synchronization with the PCO scheme, the network of nodes are able to superimpose the signals emitted by the distributed transmitters at the remote receiver. For example, we consider, in Fig. 15, UWB network with 100 nodes randomly distributed in a 100×100 m^2 area, and that each node transmits a monocycle pulse [23] where the pulse-width is 1/10 the duration of a cycle period. The transmission power of each node is set to 1 and their dynamics follow the Peskin's model with $\gamma = 4$ and $S_0 = 5$. In Fig. 15, the evolution of the superposition of signals received at a distant node is shown with the superimposed amplitude normalized by the maximum amplitude of the signal from a single node. The distance of the remote receiver is assumed to be the same for all nodes in the network. We can deduce from this figure that a cooperative transmission by synchronized transmitters allows the network to transmit to a distance 100 times further than one could reach with a single

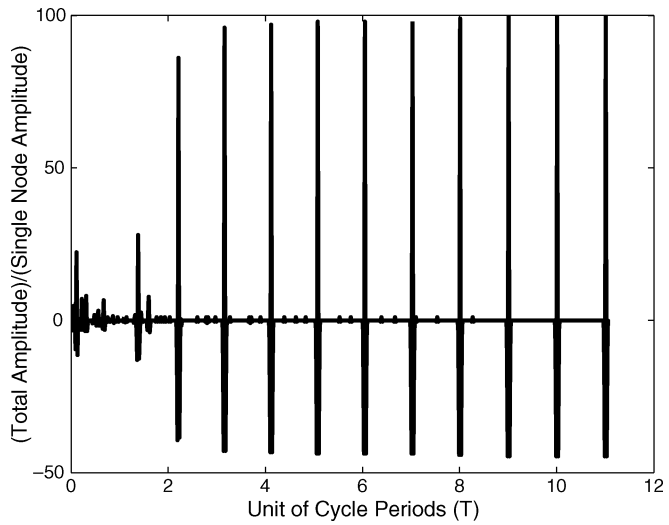

Fig. 15. Amplitude of the signal received at a far distance normalized by the maximum amplitude that one would receive if only a single node were to transmit.

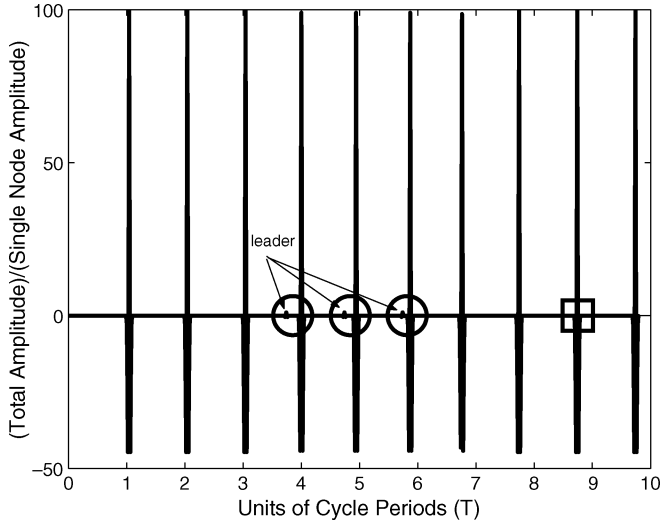

Fig. 16. Realization of the reach-back signal of the network when the information is encoded in the phase shift of the oscillator.

transmitter node when the path loss exponent $\alpha = 2$. In order to achieve the cooperative gain at the remote receiver, it is necessary for the precision of the synchronization to be within the pulse duration of the signal emitted at each node. Using the GPS to synchronize the reception at the remote destination, one can only achieve the accuracy of approximately 200 ns. it is sufficient for the sensor nodes to transmit a pulse with a duration of the same order and have a delay spread that is smaller than the pulse duration. Since the precision of the synchronization is limited by the distance of the sensors, as shown in Section VII-A, the nodes in the network should be at most 30 m apart such that the propagation delay toward the remote receiver and the maximal dispersion of the synchronization process combines for a maximum delay spread of approximately 200 ns.

With the cooperative gain shown above, we utilize the PCOs to form a *distributed modulation scheme*, similar to the traditional pulse-position modulation (PPM) scheme, that communicates over the reach-back channel. Let a node be the leader[5] of the network that is the only one that contains the data to transmit. Similar to the PPM scheme, the data symbol transmitted by the leader is represented by an offset in the pulsing time. Assume that the leader transmits a binary symbol represented by the perturbation β_0 and β_1. By incorporating this data into the dynamics of the oscillator, we modify (4) as follows:

$$\frac{dx_0(t)}{dt} = S_0 - \gamma x_0(t) + \beta_0 \delta\left[b(t)\right] + \beta_1 \delta\left[b(t) - 1\right] \quad (11)$$

where x_0 is the state of the leader node and $b(t) \in \{0, 1\}$ is now the binary data at time t. The arrival of a binary data shifts the phase of the leader by an amount depending on the parameter $\beta_{b(t)}$ which initially causes the network to go out of phase. If we restrict the leader from accepting external coupling from other PCOs, the network of nodes will progressively lock on to the phase of the leader since the leader will continuously trigger the nodes that are out of phase, while maintaining its own periodic pulsing. Once the synchronization is achieved, the aggregated signal will reach a peak in power since the signals are now added in phase, then the receiver will be able to detect the aggregated signal at a remote distance and determine the data through the phase shift in the new equilibrium. This is similar to the concept of PPM in conventional point-to-point communication systems. In this system, the leader is the only one with access to the transmitted data and act intelligently to transmit the data through (11). All the other nodes act as dumb transmitters that lock on to the pulsing of the leader. For each bit transmitted by the leader, the leader periodically emits the pulse for several cycles before the network is synchronized and, thus achieving the cooperative gain. The pulses emitted by the leader serves a dual role of conveying the information and synchronizing the network. We note that the major difference between a source and a pulse-coupled oscillator is that the source node will avoid the coupling signals from the network while still emitting a pulse, periodically, according to the oscillating mechanism.

In Fig. 16, we consider again the scenario similar to that of Fig. 15 but assume that the nodes in the network are initially synchronized. At the fourth cycle period, we impose a phase shift $\delta = 0.3$ to the current phase of the leader causing it to have a phase difference of δ with respect to the other nodes within the network. In the circles shown in Fig. 16, the small pulse next to the large aggregated signal is the offset pulse emitted by the leader. By allowing the leader to avoid the coupling from other nodes, the synchronized pulse of the other nodes will merge toward the pulse of the source node, eventually locking on to the phase of the source at the ninth cycle period, as shown in the rectangle in Fig. 16. By detecting the phase difference of the new equilibrium, with respect to the previous equilibrium, the distant receiver is able to decode the information that is cooperatively transmitted by the network.

IX. Conclusion

In this paper, we proposed a distributed synchronization protocol that is based on the simple mechanics of the pulse coupled

[5]We note that every node in the network is allowed to alternate between the role of a leader and the role of a relay.

oscillators. This method is inspired by the synchronization phenomenon that is often observed in the natural world, such as the flashing of fireflies, the firing of pacemaker cells, earthquakes, etc. We adapt to the realistic parameters of the nonideal wireless environment by including the pulse detection and the refractory period upon the original PCO model. These modifications allows the system to remain stable in synchronizing the network.

Under an idealistic model, we have shown that the convergence speed of the synchronization process decreases with the number of nodes in the network when the nodes are located within a single broadcast domain. When the transmission range of each node is limited to its near neighbors, the convergence speed, however, grows in the order of $O(\log N)$. In analyzing the energy-efficiency, we found that there exists an optimum operating point that achieves the best tradeoff between total energy consumption and synchronization time. As shown in Section VI, the transmit energy of PCO is a crucial parameter affecting not only the locking time of the synchronization, but also the total energy consumption, the robustness and the accuracy.

APPENDIX

Proof: It is easy to show that

$$\bigcap_{i=1}^{N-1} E_i \subset E_1 \Rightarrow \Pr\left\{\bigcap_{i=1}^{N-1} E_i\right\} \le \Pr\{E_1\} = 1 - e^{-\lambda\varepsilon}.$$

For the lower bound, we use the union bound as follows:

$$\begin{aligned}\Pr\left\{\bigcap_{i=1}^{N-1} E_i\right\} &= 1 - \Pr\left\{\bigcup_{i=1}^{N-1} E_i\right\} \\ &\ge \max\left\{1 - \sum_{i=1}^{N-1} \Pr\{E_i\}, 0\right\}. \qquad (12)\end{aligned}$$

From the Markov inequality, we can derive, for all i, that

$$\begin{aligned}\Pr\{E_i\} &= \Pr\{T = \tau_1 + \tau_2 + \cdots + \tau_i < i\varepsilon\} \\ &\le \frac{\mathbf{E}[e^{sT}]}{e^{si\varepsilon}} \quad \forall s > 0 \\ &= \left[\frac{\lambda e^{-s\varepsilon}}{\lambda - s}\right]^i \quad \forall s \in (0, \lambda).\end{aligned}$$

Therefore, from (12), we have

$$\begin{aligned}\Pr\left\{\bigcap_{i=1}^{N-1} E_i\right\} &\ge \max\left\{1 - \sum_{i=1}^{N-1} \Pr\{E_i\}, 0\right\} \\ &\ge \max\left\{\max_{0<s<\lambda}\left\{1 - \sum_{i=1}^{N-1}\left[\frac{\lambda e^{-s\varepsilon}}{\lambda - s}\right]^i\right\}, 0\right\} \\ &= \max\left\{1 - \sum_{i=1}^{N-1}\left[\min_{0<s<\lambda}\frac{\lambda e^{-s\varepsilon}}{\lambda - s}\right]^i, 0\right\}.\end{aligned}$$

By optimizing over the parameter s, it is easy to show that the optimum $s = \lambda - (1/\varepsilon)$ for $\lambda\varepsilon > 1$, and $s = 0$, otherwise. Therefore, we have

$$\min_{0<s<\lambda}\frac{\lambda e^{-s\varepsilon}}{\lambda - s} = \begin{cases}\lambda\varepsilon e^{-\lambda\varepsilon+1}, & \text{for } \lambda\varepsilon \ge 1 \\ 1, & \text{for } \lambda\varepsilon < 1\end{cases}. \qquad (13)$$

In conclusion, we have

$$\Pr\left\{\bigcap_{i=1}^{N-1} E_i\right\} \ge \max\{A, 0\}$$

where

$$A = \begin{cases}1 - \frac{\lambda\varepsilon e^{-\lambda\varepsilon+1} - [\lambda\varepsilon e^{-\lambda\varepsilon+1}]^N}{1 - \lambda\varepsilon e^{-\lambda\varepsilon+1}}, & \text{for } \lambda\varepsilon \ge 1 \\ -(N-2), & \text{for } \lambda\varepsilon < 1\end{cases}.$$

■

REFERENCES

[1] R. E. Mirollo and S. H. Strogatz, "Synchronization of pulse-coupled biological oscillators," *SIAM J. Appl. Math.*, vol. 50, no. 6, pp. 1645–1662, Dec. 1990.

[2] A. El-Hoiydi, "Spatial TDMA and CSMA with preamble sampling for low power ad hoc wireless sensor networks," in *Proc. IEEE Int. Symp. Comput. Commun. (ISCC)*, Jul. 2002, pp. 685–692.

[3] T. Salonidis, P. Bhagwat, L. Tassiulas, and R. LaMaire, "Distributed topology construction of Bluetooth personal area networks," in *Proc. IEEE INFOCOM*, Apr. 2001, pp. 1577–1586.

[4] Y.-W. Hong and A. Scaglione, "On multiple access for correlated sources: A content-based group testing approach," presented at the IEEE Inf. Theory Workshop, San Antonio, TX, Oct. 2004.

[5] ——, "Content-based multiple access: Combining source and multiple access coding for sensor networks," presented at the Proc. IEEE Int. Workshop Multimedia Signal Process., Siena, Italy, Sep. 2004.

[6] S. Ganeriwal, R. Kumar, S. Adlakha, and M. B. Srivastava, "Network-wide time synchronization in sensor networks," NESL, Tech. Rep., 2003.

[7] J. Elson, L. Girod, and D. Estrin, "Fine-grained network time synchronization using reference broadcasts," presented at the 5th Symp. Operating Syst. Design, Implement. (OSDI), Dec. 2002.

[8] K. Römer, "Time synchronization in ad hoc networks," in *Proc. 2nd ACM Int. Symp. Mobile Ad Hoc Netw. Comput.*, 2001, pp. 173–182.

[9] L. Glass and M. C. Mackey, *From Clocks to Chaos: The Rhythms of Life*. Princeton, NJ: Princeton Univ. Press, 1988.

[10] Y. Kuramoto, *Chemical Oscillations, Waves and Turbulence*. Berlin, Germany: Springer-Verlag, 1984.

[11] J. Buck and E. Buck, "Synchronous fireflies," *Scientific Amer.*, vol. 234, pp. 74–85, 1976.

[12] L. F. Abbott, "A network of oscillators," *J. Phys. A, Math. Gen.*, vol. 23, pp. 3835–3859, 1990.

[13] U. Ernst, K. Pawelzik, and T. Geisel, "Delay-induced multistable synchronization of biological oscillators," *Phy. Rev. E*, vol. 57, no. 2, pp. 2150–2162, Feb. 1998.

[14] W. Gerstner, "Rapid phase locking in systems of pulse-coupled oscillators with delays," *Phys. Rev. Lett.*, vol. 76, no. 10, pp. 1755–1758, Mar. 1996.

[15] A. Scaglione and Y.-W. Hong, "Opportunistic large arrays: Cooperative transmission in wireless multihop ad hoc networks for the reach back channel," *IEEE Trans. Signal Process.*, vol. 51, no. 8, pp. 2082–2092, Aug. 2003.

[16] S. Campbell, D. Wang, and C. Jayaprakash, "Synchrony and desynchrony in integrate-and-fire oscillators," *Neural Comput.*, vol. 11, pp. 1595–1619, 1999.

[17] J. Elson and K. Römer, "Wireless sensor networks: A new regime for time synchronization," *ACM SIGCOMM Comput. Commun. Rev.*, vol. 33, no. 1, pp. 149–154, Jan. 2003.

[18] M. Z. Win and R. A. Scholtz, "Ultra-wide bandwidth time-hopping spread spectrum impulse radio for wireless multiple-access communications," *IEEE Trans. Commun.*, vol. 48, no. 4, pp. 679–689, Apr. 2000.

[19] J. Mannermaa, K. Kalliomaki, T. Mansten, and S. Turunen, "Timing performance of various GPS receivers," in *Proc. Joint Meeting Eur. Freq. Time Forum and IEEE Int. Freq. Control Symp.*, Apr. 1999, pp. 287–290.

[20] D. L. Mills, "Internet time synchronization: The network time protocol," *IEEE Trans. Commun.*, vol. 39, no. 10, pp. 1482–1493, Oct. 1991.

[21] M. B. H. Rhouma and H. Frigui, "Self-organization of pulse-coupled oscillators with applications to clustering," *IEEE Trans. Pattern Anal. Machine Intell.*, vol. 23, no. 2, pp. 180–195, Feb. 2001.

[22] C. S. Peskin, *Mathematical Aspects of Heart Physiology*. New York: New York University, 1975. Courant Institute Mathematical Science.

[23] M. Z. Win and R. A. Scholtz, "Ultra-wide bandwidth time-hopping spread spectrum impulse radio for wireless multiple-access communications," *IEEE Trans. Commun.*, vol. 48, no. 4, pp. 679–691, Apr. 2000.
[24] R. Mathar and J. Mattfeldt, "Pulse-coupled decentral synchronization," *SIAM J. Applied Mathematics*, vol. 56, no. 4, pp. 1094–1106, Aug. 1996.

Yao-Win Hong (S'01) received the B.S. degree in electrical engineering from National Taiwan University, Taipei, Taiwan, in 1999. He is currently working towards the Ph.D. degree in the School of Electrical and Computer Engineering, Cornell University, Ithaca, NY.

His research is focused on low complexity network protocols, source coding/multiple-access channel coding problems for sensor networks and physical layer designs for multihop ad hoc networks.

Anna Scaglione (S'97–M'99) received the "Laurea" and Ph.D. degrees in electrical engineering from the University of Rome "La Sapienza," Rome, Italy, in 1995 and 1999, respectively.

She was Postdoctoral Research Affiliate at the University of Minnesota, Minneapolis, from 1999 to 2000. Since 2001, she has been an Assistant Professor of Electrical Engineering at Cornell University, Ithaca, NY. Prior to this, she was an Assistant Professor during the academic year 2000–2001 at the University of New Mexico, Albuquerque, NM. Her research is in the broad area of signal processing for communication systems. Her current research focuses on optimal transceiver design for MIMO-broadband systems and cooperative communications systems for large scale sensor networks.

Dr. Scaglione received the 2000 IEEE Signal Processing Transactions Best Paper Award and the National Science Foundation (NSF) Career Award in 2002. She was recently nominated as a member of the IEEE Signal Processing for Communication Technical Committee. She is an Associate Editor for the IEEE TRANSACTIONS ON WIRELESS COMMUNICATIONS and has been Co-Guest Editor of the *Communication Magazine* Special Issue on Power Line Communications "Broadband is Power: Internet Access Through the Power Line Networks," May 2003.